

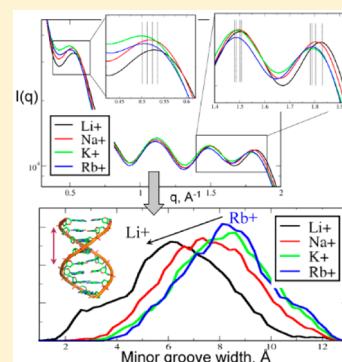
Differential Impact of the Monovalent Ions Li^+ , Na^+ , K^+ , and Rb^+ on DNA Conformational Properties

Alexey Savelyev and Alexander D. MacKerell, Jr.*

Department of Pharmaceutical Sciences, School of Pharmacy, University of Maryland, 20 Penn Street, Room 629, Baltimore, Maryland 21201, United States

Supporting Information

ABSTRACT: The present report demonstrates that the conformational properties of DNA in solution are sensitive to the type of monovalent ion. Results are based on the ability of a polarizable force field using the classical Drude oscillator to reproduce experimental solution X-ray scattering data more accurately than two nonpolarizable DNA models, AMBER Parmbsc0 and CHARMM36. The polarizable model is then used to calculate scattering profiles of DNA in the presence of four different monovalent salts, LiCl , NaCl , KCl , and RbCl , showing the conformational properties of DNA to vary as a function of ion type, with that effect being sequence-dependent. The primary conformational mode associated with the variations is contraction of the DNA minor groove width with decreasing cation size. These results indicate that the Drude polarizable model provides a more realistic representation of ion–DNA interactions than additive models that may lead to a new level of understanding of the physical mechanisms driving salt-mediated biological processes involving nucleic acids.



Conformational characterization of DNA in solution still remains a challenge, including understanding the impact of ion type on structural and dynamical properties. While X-ray crystallography and solution NMR are the primary tools used to experimentally study DNA structure,¹ there are limitations on their ability to fully represent DNA conformational properties in solution. In the case of X-ray crystallography, the DNA molecule is subject to crystal packing forces, which may affect its local and global geometric characteristics.^{2,3} Solution NMR is often limited in its ability to model the overall DNA conformation, and structure refinement depends on the underlying mathematical framework,⁴ which may lead to conflicting structural models. Alternatively, a solution technique, X-ray diffraction “fingerprinting”, is capable of differentiating between the conflicting crystallographic and NMR DNA structures⁵ and can serve as a robust tool for the evaluation of the quality of computational models used to investigate DNA.⁶ This technique differs from X-ray crystallography in that the solution scattering pattern represents a concise but faithful representation of the full range of DNA dynamics in solution in terms of a limited number of dominant macromolecular conformational modes (1D “fingerprint”), with finer details being averaged over, a concept very similar to the way the complex multidimensional landscape of a protein in its native state is reduced to several essential energetic basins of low dimensionality.⁷ Therefore, the information content of solution scattering data allows for unique insights into DNA conformational properties in solution as well as being of utility for the validation of empirical force fields.

In the current study, the recently developed polarizable force field for DNA based on the classical Drude oscillator model^{8,9} is shown to quantitatively reproduce the experimentally measured

solution-state X-ray diffraction profiles of a number of B form DNA sequences.⁵ This contrasts results from two commonly used computational atomistic DNA force fields, the state-of-the-art additive CHARMM36 (C36)¹⁰ and AMBER Parmbsc0¹¹ models, with respect to their ability to capture the essential DNA conformational properties in solution. In addition, simulated spectra of DNA solvated in aqueous solutions containing different monovalent salts, LiCl , NaCl , KCl , and RbCl , address an important question in the field of DNA biophysics: are differential effects of ion type present and how strong are those effects on DNA conformational properties? Because DNA under physiological conditions is exposed to a mixture of several (mono- and divalent) ionic species, it is important to understand the impact of those ions individually on DNA structure. Studies to date on this topic are limited. Experiments on the compaction of T4 DNA have shown differential effects of monovalent ions;¹² however, no data are available on the differential impact of ion type on small DNA molecules, a necessary step required to understand ion effects in more complex systems. As we report, the type of monovalent ion does impact the solution conformational properties of DNA as observed in MD simulations using a force field that includes the explicit treatment of electronic polarizability using the classical Drude oscillator model. This represents an experimentally untested prediction of the model that is anticipated to set the foundation for further experimental and computational studies of the impact of ion type on DNA conformational properties, information that will help us to

Received: November 20, 2014

Accepted: December 19, 2014

Published: December 22, 2014

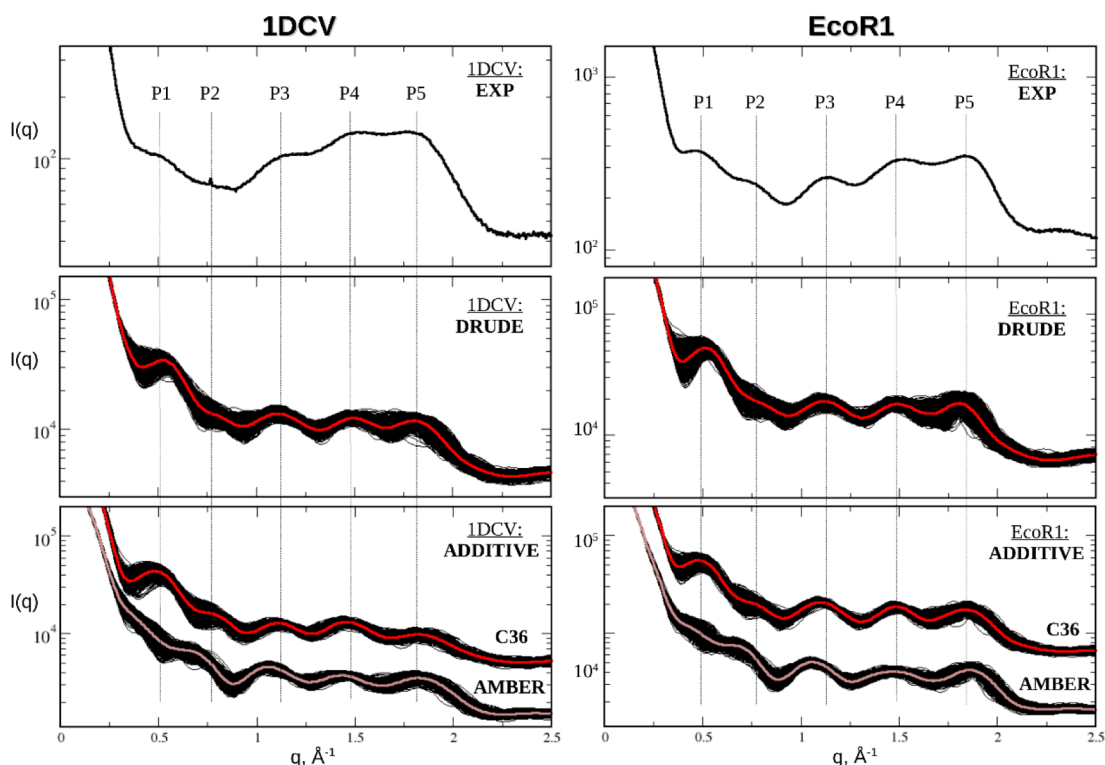


Figure 1. Solution scattering profiles for the 1DCV and *EcoRI* systems from the experiments (upper row) and computed from MD simulations utilizing Drude polarizable (middle row) and additive CHARMM36 and AMBER Parmbsc0 (lower row) DNA models solvated in ~100 mM NaCl ionic buffer. Positions of the experimental peaks are projected onto the computational results. Intensities for the additive AMBER and C36 systems are shifted with respect to each other to facilitate their comparison.

better understand issues such as competitive ionic binding to DNA,¹³ salt-driven nucleic acid array condensation,¹⁴ and other salt-mediated biological processes involving DNA.

Because of the dynamics of DNA in solution, a typical solution X-ray diffraction pattern represents a collection of diffuse peaks, whose number, breadth of dispersion, and positions are unique for a particular sequence. The orientational averaging allows the intensity of molecular scattering to be represented by a mathematically tractable formula in which all vectorial quantities (wave-vector and radius-vector) are reduced to their scalar values. (See the Supporting Information, SI, for details.) Intensities at small wave numbers contain information on the overall shape and size of DNA in solution, while those at higher wave numbers provide structural details arising from spatially resolved atomic correlations within the macromolecule. For example, on the basis of decomposition of the molecular DNA structure into the nucleic acid bases and sugar–phosphate backbones, it was demonstrated that the last major peak of the spectra (at $q \approx 1.7$ to 2.1 \AA^{-1}) corresponds primarily to the geometry of the base pair stacking, while the spectral pattern in the range of $q \approx 0.2$ to 1.7 \AA^{-1} reflects the combined contribution from the sugar and phosphate moieties.^{5,6}

Presented in Figure 1 are solution scattering profiles for two self-complementary B form DNA sequences, d(CGCGAA-TTCGCG)2 and d(CGCTAGCG)2 from experiments⁵ and MD simulations utilizing the Drude polarizable and additive C36 and AMBER Parmbsc0 force fields. In what follows, we refer to these molecules as *EcoRI* and 1DCV, respectively. The first structure is also known as the Drew–Dickerson dodecamer, one of the most studied DNA sequences to date.¹⁵

The second, 1DCV, is a 10-base-pair crystal structure¹⁶ that contains one extra base pair at each termini as compared with the sequence studied in solution scattering experiments.⁵ To be consistent with those experiments, only the internal eight base pairs of 1DCV were used in the calculation of the spectra. (See the SI for details on MD simulation protocols.) As seen in Figure 1, the Drude polarizable and C36 additive models generate scattering spectra consistent with experiment for both systems studied, with the number of peaks (P1–P5) and their approximate positions corresponding to those observed experimentally. In contrast, the AMBER profiles lack a discernible first peak for both systems, with the position of the rest of peaks deviating from experimental positions. For a more quantitative comparison, the peak positions were determined and rms deviations computed between the experimental and simulation results (Table 1). The best agreement with experiment occurs with the Drude model, followed by the additive C36 model, with the AMBER results deviating the most. Discrepancies between experiment and MD simulations of *EcoRI* were observed previously in a previous AMBER DNA force field,⁶ where an analogous mismatch in the peak positions and the failure to generate the first major scattering peak (P1) occurred. The scattering results correlate with the magnitudes of structural rms differences (rmsd) of the 1DCV and *EcoRI* molecules with respect to ideal B form DNA (see Figure S1A, SI). In particular, the largest rmsd's are generated by the AMBER force field, with lesser values obtained for the C36 and Drude models. Additionally, a visual comparison of the structures from the Drude, C36, and AMBER simulations reveals significant differences in the overall shape of the macromolecule (see Figure S1B, SI), consistent with the observed differences in the scattering profiles.

Table 1. Peak Positions Inferred from Experimental and Computational Solution Scattering Profiles

peak	EXP	MD ^a		
		C36	AMBER	DRUDE
EcoRI, 12 base pairs				
P1	0.456	0.442		0.507
P2	0.750 ^b	0.800 ^b	0.640 ^b	0.785 ^b
P3	1.127	1.101	1.055	1.117
P4	1.513	1.478	1.472	1.490
P5	1.834	1.829	1.861	1.803
rmsd (P2 – P5)		0.033	0.084	0.018
rmsd_all		0.030		0.027
IDCV, 10 base pairs ^c				
P1	0.510	0.480		0.520
P2	0.755 ^d	0.800 ^d	0.700 ^d	0.820 ^d
P3	1.180	1.100	1.050	1.110
P4	1.525	1.455	1.435	1.495
P5	1.790	1.825	1.830	1.800
rmsd (P2 – P5)		0.060	0.086	0.050
rmsd_all		0.055		0.045

^aPeak positions were determined from zero crossing points in the first derivative; values are in Å⁻¹. ^bApproximate positions of the plateau at P2. ^cOnly internal eight base pairs were considered to be consistent with the experimentally studied sequence. ^dApproximate positions of the spike at P2.

The above results were obtained for DNA molecules solvated in an ~100 mM NaCl aqueous buffer. However, the experimental conditions contained an additional ~50 mM Tris·HCl.⁵ Therefore, we repeated the additive C36 MD simulations of *EcoRI* and 1DCV molecules immersed in a ~100 mM NaCl with ~50 mM Tris·HCl aqueous buffer and

recomputed the DNA scattering profiles to find out if the altered conditions affect the results. As shown in the Figure S2 of SI, the presence of Tris·HCl did not lead to any noticeable differences in the spectra.

A more intriguing picture emerges when ion type is altered from Na⁺ to other monovalent ionic species, including Li⁺, K⁺, and Rb⁺. Figure 2 shows scattering profiles for 1DCV and *EcoRI* simulated in LiCl, NaCl, KCl, and RbCl aqueous buffers using the Drude polarizable and C36 additive force fields. The striking observation is that the Drude polarizable model predicts the different ions to alter the conformational properties of the DNA. Such variation is not present with the additive C36 force field, a result that was also obtained with AMBER for 1DCV (not shown). Among all spectral peaks, the biggest variation is observed for the first (P1) and the two last major peaks (P4, P5), indicating that both local and global DNA geometric parameters are affected. Structural analysis identified significant variation in the minor groove width as a function of ion type (see Figure 3 and Table S1, SI). In addition, some helicoidal parameters demonstrated variations (see Figure S3, SI). Interestingly, no significant variability of the major groove width with ion type was observed (see Figure S4, SI).

Notably, the extent of the variations is much larger for 1DCV versus *EcoRI*, which may indicate that the observed effect is sequence-specific. To address this possibility, we performed a similar analysis on an additional sequence, d(CGCATGCTA-CGC), a structure recently resolved by solution NMR (PDB: 2L8Q).¹⁷ This sequence is the same length as *EcoRI* but does not possess an AATT-tract. The solution spectra for all four ionic buffers and the minor groove width distributions are shown in the Figure S5 in the SI and Figures 3E,F, respectively. Additionally, distributions for selected helicoidal parameters affected the most by the changes in ionic environment are

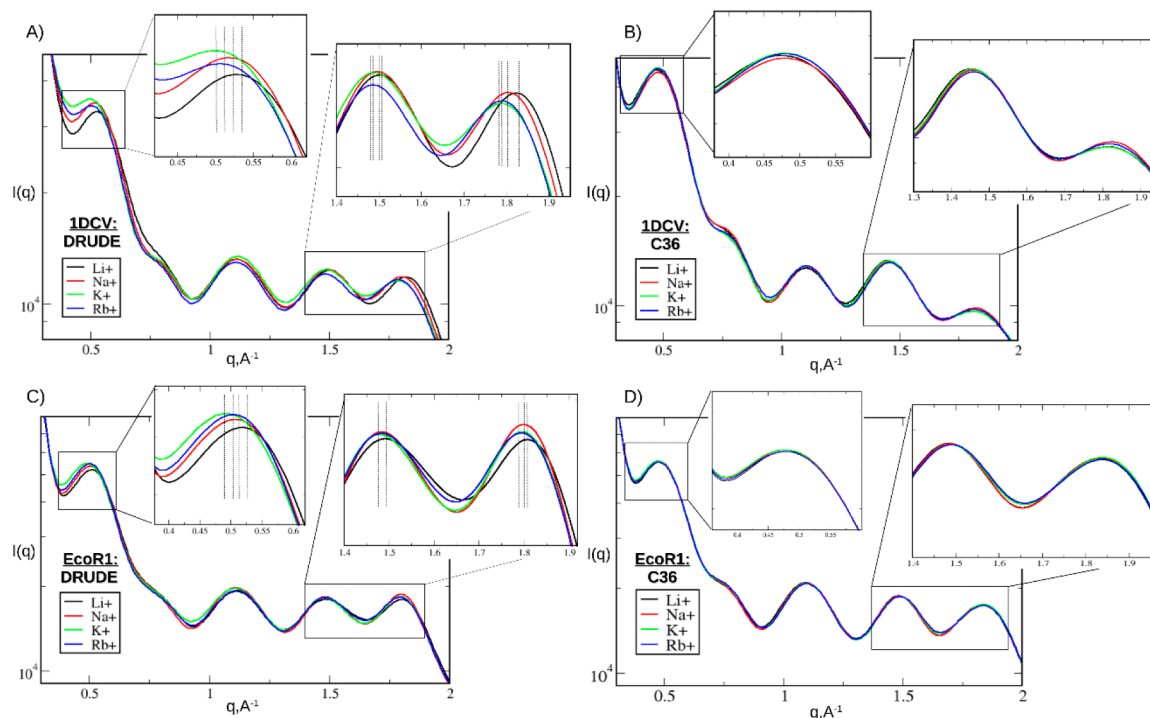


Figure 2. Solution scattering profiles computed from the Drude polarizable (A,C) and CHARMM36 additive (B,D) MD simulations of the 1DCV and *EcoRI* DNA sequences solvated in LiCl, NaCl, KCl, and RbCl containing aqueous buffers. For the Drude model demonstrating spectral variability with the ion type, the approximate positions of the first and two last peaks are schematically shown.

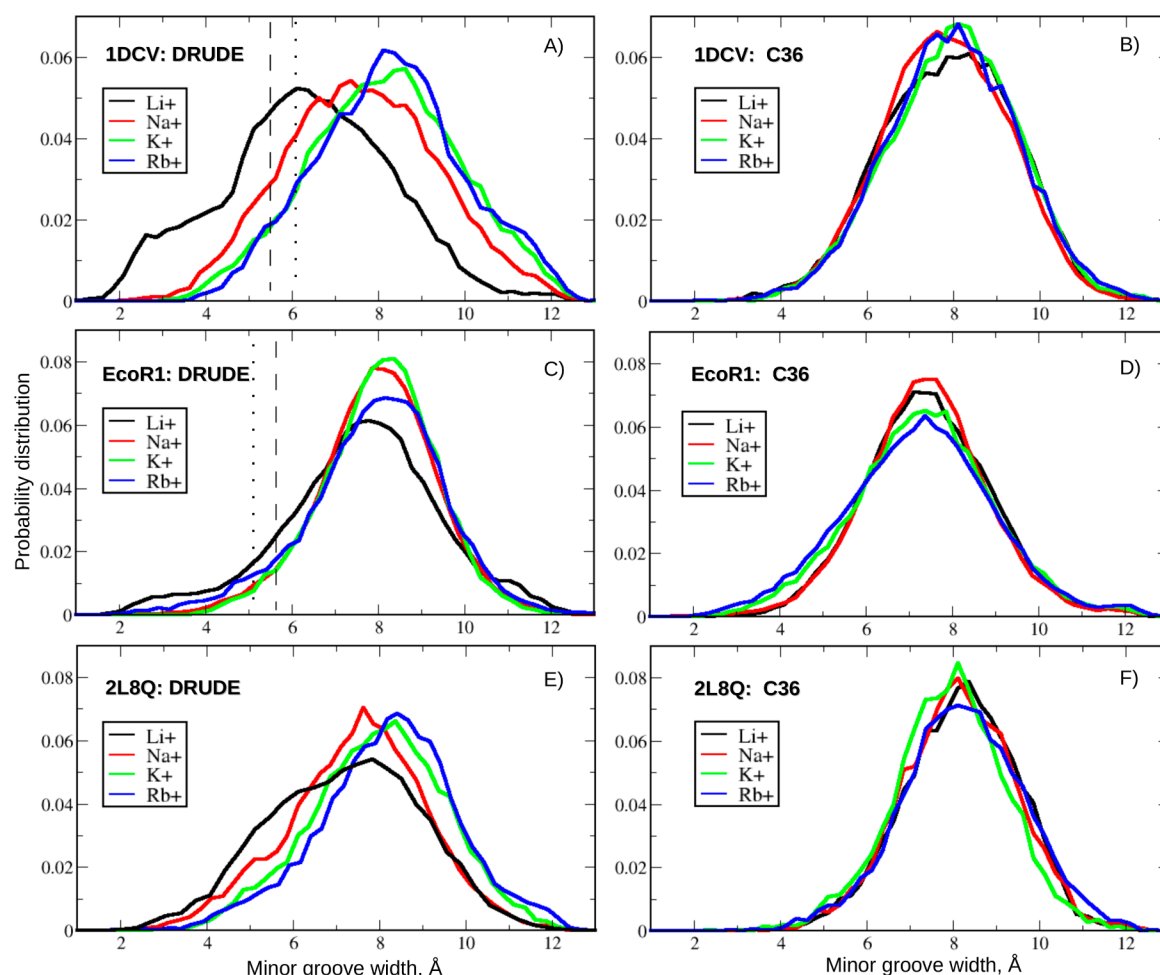


Figure 3. Probability distributions for the minor groove width computed from the Drude polarizable and additive CHARMM36 MD simulations of the 1DCV, *EcoRI*, and 2L8Q DNA systems solvated in various monovalent ionic buffers. For comparison, estimates of the minor groove width inferred from selected NMR (PDB for 1DCV: 1G80; PDB for *EcoRI*: 1DUF) and crystallographic (PDB for 1DCV: 2S0D; PDB for *EcoRI*: 1BNA) structures are shown in panels A and C as dashed and dotted lines, respectively.

shown in the Figure S3 in the SI. 2L8Q demonstrates an intermediate propensity for its conformation to change due to the different ions relative to *EcoRI* and 1DCV, with the trend remaining the same for the changes in the spectral patterns, the minor groove width, and selected helicoidal parameters. The general feature observed in all systems is that the DNA spectral profiles are uniformly shifted to higher values of the scattering vector as a function of ion size with $\text{Rb}^+ < \text{K}^+ < \text{Na}^+ < \text{Li}^+$. The minor groove width is the structural feature correlating the most with the spectral changes, although variations in translational and rotational helicoidal parameters, such as tilt, roll, twist, propeller twist, and shift, also contribute to the overall picture. These results indicate a decrease in the minor groove width for the above series. Additional analyses of the structural changes along with molecular details of specific interactions involving the ions are ongoing and will be reported in a future study.

The present findings as well as the results based on prior computational studies utilizing Drude polarizable DNA model^{9,18} indicate that inclusion of polarization effects indeed provides more realistic representation of the many-body effects in the DNA polyion and the interactions of DNA with its ionic environment. The differences in conformational properties as a function of ion type predicted by the model are notable, with

those effects being sequence-dependent. To date, no experimental scattering studies of the role of ion type on DNA conformation have been performed. Thus, these results prompt for additional solution-scattering experiments involving more DNA sequences and ionic buffers. In this light, Drude polarizable MD simulations may offer the potential to yield new insights into salt-mediated biological processes involving DNA, such as protein–DNA recognition and chromatin folding.

■ ASSOCIATED CONTENT

Supporting Information

MD simulation protocols, implementation of the routing calculating solution scattering profiles from MD simulations, description of the DNA structural analysis, and supplementary figures and tables. This material is available free of charge via the Internet at <http://pubs.acs.org>.

■ AUTHOR INFORMATION

Corresponding Author

*E-mail: alex@outerbanks.umaryland.edu. Phone: (410) 706-7442. Fax: (410) 706-5017.

Notes

The authors declare no competing financial interest.

■ ACKNOWLEDGMENTS

We acknowledge the NIH (GM051501) for financial support and the University of Maryland Computer-Aided Drug Design Center and the XSEDE resources for their generous allocations of computer time. We thank Dr. Xiaobing Zuo for providing experimental solution scattering data used in this study and Drs. Nathan Baker, Alexey Onufriev, and Marc Taraban for helpful discussions.

■ REFERENCES

- (1) Berman, H. M.; Olson, W. K.; Beveridge, D. L.; Westbrook, J.; Gelbin, A.; Demeny, T.; Hsieh, S.-H.; Srinivasan, A. R.; Schneider, B. The Nucleic Acid Database: A Comprehensive Relational Database of Three-Dimensional Structures of Nucleic Acids. *Biophys. J.* **1992**, *63*, 751–759.
- (2) Abrescia, N. G. A.; Thompson, A.; Huynh-Dinh, T.; Subirana, J. A. Crystal Structure of an Antiparallel DNA Fragment with Hoogsteen Base Pairing. *Proc. Natl. Acad. Sci. U.S.A.* **2002**, *99*, 2806–2811.
- (3) Abrescia, N. G. A.; Gonzalez, C.; Gouyette, C.; Subirana, J. A. X-ray and NMR Studies of the DNA Oligomer d(ATATAT): Hoogsteen Base Pairing in Duplex DNA. *Biochemistry* **2004**, *43*, 4092–4100.
- (4) Kuszewski, J.; Schwieters, C.; Clore, G. M. Improving the Accuracy of NMR Structures of DNA by Means of a Database Potential of Mean Force Describing Base-Base Positional Interactions. *J. Am. Chem. Soc.* **2001**, *123*, 3903–3918.
- (5) Zuo, X. B.; Tiede, D. M. Resolving Conflicting Crystallographic and NMR Models for Solution-State DNA with Solution X-ray Diffraction. *J. Am. Chem. Soc.* **2005**, *127*, 16–7.
- (6) Zuo, X. B.; Cui, G. L.; Merz, K. M.; Zhang, L. G.; Lewis, F. D.; Tiede, D. M. X-ray Diffraction “Fingerprinting” of DNA Structure in Solution for Quantitative Evaluation of Molecular Dynamics Simulation. *Proc. Natl. Acad. Sci. U.S.A.* **2006**, *103*, 3534–3539.
- (7) Materese, C. K.; Goldmon, C. C.; Papoian, G. A. Hierarchical Organization of Eglin C Native State Dynamics is Shaped by Competing Direct and Water-Mediated Interactions. *Proc. Natl. Acad. Sci. U.S.A.* **2008**, *105*, 10659–10664.
- (8) Savelyev, A.; MacKerell, A. D., Jr. All-Atom Polarizable Force Field for DNA Based on the Classical Drude Oscillator Model. *J. Comput. Chem.* **2014**, *35*, 1219–1239.
- (9) Savelyev, A.; MacKerell, A. D., Jr. Balancing the Interactions of Ions, Water, and DNA in the Drude Polarizable Force Field. *J. Phys. Chem. B* **2014**, *118*, 6742–6757.
- (10) Hart, K.; Foloppe, N.; Baker, C. M.; Denning, E. J.; Nilsson, L.; MacKerell, A. D., Jr. Optimization of the CHARMM Additive Force Field for DNA: Improved Treatment of the BI/BII Conformational Equilibrium. *J. Chem. Theory Comput.* **2012**, *8*, 348–362.
- (11) Pérez, A.; Marchán, I.; Svozil, D.; Sponer, J.; Cheatham, T. E., III; Laughton, C. A.; Orozco, M. Refinement of the AMBER Force Field for Nucleic Acids: Improving the Description of alpha/gamma Conformers. *Biophys. J.* **2007**, *92*, 3817–3829.
- (12) Zinchenko, A. A.; Yoshikawa, K. Na⁺ Shows a Markedly Higher Potential than K⁺ in DNA Compaction in a Crowded Environment. *Biophys. J.* **2005**, *88*, 4118–4123.
- (13) Bai, Y.; Greenfeld, M.; Travers, K. J.; Chu, V. B.; Lipfert, J.; Doniach, S.; Herschlag, D. Quantitative and Comprehensive Decomposition of the Ion Atmosphere Around Nucleic Acids. *J. Am. Chem. Soc.* **2007**, *129*, 14981–14988.
- (14) Tolokh, I. S.; Pabit, S. A.; Katz, A. M.; Chen, Y.; Drozdetski, A.; Baker, N.; Pollack, L.; Onufriev, A. V. Why Double-Stranded RNA Resists Condensation. *Nucleic Acids Res.* **2014**, *42*, 10823–10831.
- (15) Drew, H. R.; Wing, R. M.; Takano, T.; Broka, C.; Tanaka, S.; Itakura, K.; Dickerson, R. S. Structure of a B-DNA dodecamer: Conformation and Dynamics. *Proc. Natl. Acad. Sci. U.S.A.* **1981**, *78*, 2179–2183.
- (16) Eichman, B. F.; Vargason, J. M.; Mooers, B. H. M.; Ho, P. S. The Holliday Junction in an Inverted Repeat DNA Sequence: Sequence Effects on the Structure of Four-Way Junctions. *Proc. Natl. Acad. Sci. U.S.A.* **2000**, *97*, 3971–3976.
- (17) Julien, O.; Beadle, J. R.; Magee, W. C.; Chatterjee, S.; Hostetler, K. Y.; Evans, D. H.; Sykes, B. D. Solution Structure of a DNA Duplex Containing the Potent Anti-Poxvirus Agent Cidofovir. *J. Am. Chem. Soc.* **2011**, *133*, 2264–2274.
- (18) Lemkul, J. A.; Savelyev, A.; MacKerell, A. D., Jr. Induced Polarization Influences the Fundamental Forces in DNA Base Flipping. *J. Phys. Chem. Lett.* **2014**, *5*, 2077–2083.